INVESTIGATING THE ROLE OF SnO_2/ZnO BILAYER FILMS AS ELECTRON TRANSPORT LAYERS IN PEROVSKITE SOLAR CELLS

Nan Htet Htet Oo[1], Zin Min Myat[2], Zin Min Tun[3], Yin Maung Maung[4]

Abstract

This study focuses on the structural, chemical, and optical properties of SnO_2/ZnO films, prepared through sol-gel and spin-coating techniques on FTO-coated glass substrates. The research employs X-ray Diffraction (XRD) for crystalline structure analysis, Fourier Transform Infrared Spectroscopy (FTIR) for material verification, and UV-Vis spectroscopy to examine optical properties and energy band gaps. The presented approach demonstrates an efficient and cost-effective method for producing approving SnO_2/ZnO ETLs in perovskite-based quantum dot solar cells.

Keywords: SnO_2 /ZnO, ETL, XRD, FTIR, UV and perovskite solar cell

Introduction

The perovskite solar cells (PSCs) have recently gained major attention as potentially useful photovoltaic technology due to their ever-increasing power-conversion efficiency (PCE). The efficiency of PSCs depends strongly on the type of materials selected as the electron transport layer (ETL). Material selection is the foundation of all engineering applications and designs. This selection process can be defined by application requirements, possible materials, physical principles, and selection (M. Karolus, et al.,2023). In the past few years, SnO_2 is an important n-type wide-energy-gap semiconductor (Eg = 3.64 eV, 330 K) which has a wide range of applications such as in solid-state gas sensors, transparent conducting electrodes (Chopra, K.L., Major, S., et al.,1983), rechargeable Li batteries (Peng, Z., Shi, Z., Liu, M., et al,2000), and optical electronic devices (Aoki, A., Sasakura, H.: et al.,1970). During the past decade, SnO_2 nanostructures have been one of the most important oxide nanostructures due to their properties and potential applications. Many processes have been developed to the synthesis of SnO_2 nanostructures, e.g., spray pyrolysis (Paraguay-Delgado, F., et al.,2005) hydrothermal methods, evaporating tin grains in air (Duan, J., Yang, S., ei al.,2005), chemical vapor deposition, thermal evaporation of oxide powders, rapid oxidation of elemental tin, the sol–gel method, etc. The sol-gel method is one of the most promising because it is relatively simple process that enables straight-forward control of thin film properties. Kim et al. reported that films prepared using sol gel methods were suitable for device applications. The Controlling the size and shape of nanostructures can affect their electrical and optical properties (Cheng, B., Russell, J.M., ei al.,2004). The sol-gel method has many advantages over hybrid organic-organic materials that do not exist in nature (Liu, Y., Koep, E., Liu, M.: ei al.,2006). In addition, it is a low-cost and large-area processing technique. In this study, SnO2 films were prepared by Sol-Gel Spin Coating Method (SGSC) with SnCl2.2H2O (Dai, Z.R., Gole, J.L., ei al.,2002). Most high-performance PSCs are fabricated using the spin-coating method, which has better control over film thickness, quality, and machinability of the substrates, as well as dynamic spinning, hot-casting, anti-solvent annealing, Other methods such as gas and vacuum-quenching, facile spin-coating techniques, etc., are likely to be used to fabricate high-quality perovskite films (. Tin oxide is one of the best metal oxide materials for use as an electron transport layer (ETL) in PSCs. Among all the candidates, SnO2 stands out as one of the best candidates for ETL due to its wide optical band gap (3.6–4.0 eV), deep bandgap, high electron-to-electron (V-10) s-1), long carrier diffusion length, excellent chemical stability, and ease of preparation (via solution processing) at

[1] Department of Physics, University of Yangon
[2] Department of Physics, West Yangon University
[3] Department of Physics, West Yangon University
[4] Department of Physics, University of Yangon

low temperatures (Pourfayaz, F., et al.,2005). Due to its solution processing, SnO2 offers low production cost, flexibility, It can bring advantages such as easy scaling, and additive manufacturing processes (20.0.0). However, ZnO is a promising candidate due to its high transparency, suitable energy band structure, and high electron mobility. The influence of ZnO structures with different weight percentages on photovoltaic performance was investigated. The choice of SnO2 /ZnO is related to the low temperature required for their synthesis and their properties, in particular, Lamfred. F.C. Raghuwanshi, ei al.,2015).

Materials and Methods

Experimental Procedure of Tin Oxide (SnO_2) Films

Starting materials such as tin chloride dihydrates ($SnCl_2.2H_2O$) and ethanol (CH_3CH_2OH) were of analytical grade and used without further purification. The methods used in this research work were sol-gel and spin coating. The tin oxide films were prepared using $SnCl_2.2H_2O$ and ethanol by sol-gel method. In a typical experiment, different molar concentration of (0.01M-0.05M) of $SnCl_2.2H_2O$ was dissolved with 40 ml of ethanol under magnetic stirring at 1000 rpm for 5 h to form a homogeneous solution at room temperature. The experiment was prepared five times for five different molar concentrations and then, the stirring temperature was improved at 70 º C for 2 h to form a sol-gel. Afterward, the sol-gel solution was kept overnight at room temperature. Then the precursor solutions were coated onto the fluorine doped tin oxide (FTO) glass substrates by direct spin coating method. Before coating, firstly, the 1 cm × 1 cm FTO glass substrates were cleaned with distilled water and dried at room temperature and then, they were also immersed in a solution of ethanol and acetone for 15 min respectively and dried at room temperature. The cleaning glass substrates were tested the conducting layers with digital meter. The precursor solution of five different molarities was spin coated on a glass substrate at 3000 rpm for 30 s. After spin coating, glass substrates were dried at 100º C for 30 min. the prepared films were annealed at 500º C for 1 h respectively. The block diagram of preparation of tin oxide films were shown in figure 1. Figure 2 (a-d) showed the photos of preparation of tin oxide (SnO_2) films.

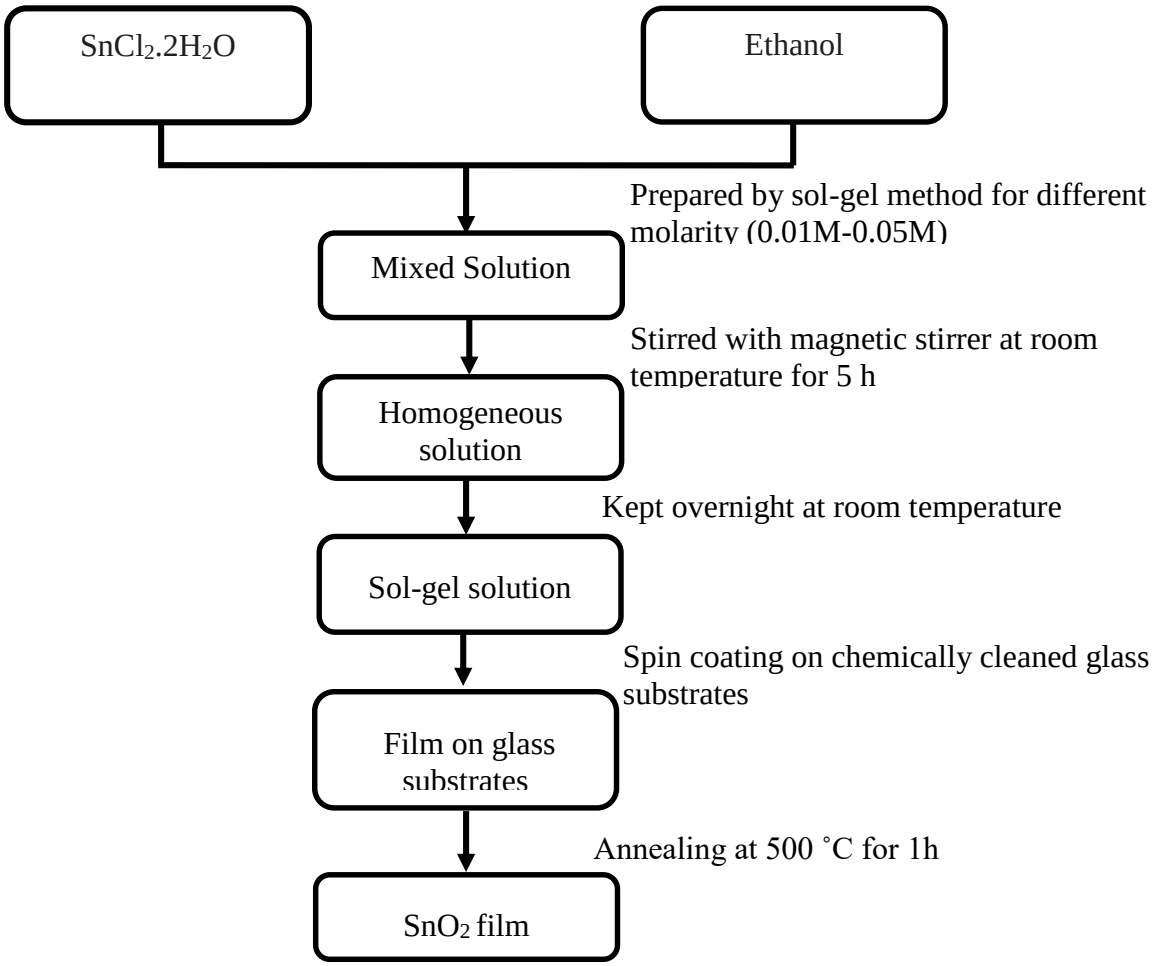

Figure 1 The block diagram of preparation of tin oxide film

Figure 2 (a) Stirring process

Figure 2 (b) Sol-gel solution

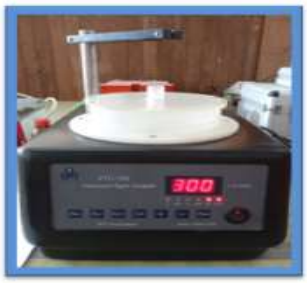

Figure 2 (c) Spin coating process

Figure 2 (d) Annealing process

Synthesized Method of ZnO and Device Fabrication of FTO/SnO_2/ZnO Films

Zinc Oxide nanostructure was synthesized by using sol-gel method. Firstly 20.83 g of $ZnCl_2.4H_2O$ and 4g of Sodium Hydroxide (NaOH) were weighted using a weighting balance. Then 100 ml of deionized water was measured by a measuring cylinder two times. After that, 20.83 g of $ZnCl_2.4H_2O$ was dissolved with a 100 ml of deionized water and 4 g of Sodium Hydroxide (NaOH) was dissolved in a 100 ml of deionized water. The solutions were stirred with a magnetic stirrer for 15 minutes each. After well mixed, sodium hydroxide solution was poured to the solution containing $ZnCl_2.4H_2O$ with a constant stirring by magnetic stirrer at 80ºC for 3 hours. After the reaction, white color sol-gel was formed. Then this solution was spin coated on the FTO/ SnO_2 glass substrates at 3000 rpm for 30 s. After that, FTO/SnO_2/ZnO glass substrates were dried at 100 ºC for 30 min. These prepared films were annealed at 500 ºC for 1 h. Finally, the fabrication of SnO_2/ZnO bilayers as electron transporting layers in perovskite solar cells was successfully observed. Figure 3 showed the block diagram of experimental procedure of ZnO and device fabrication FTO/SnO_2/ZnO films. The structural, function group and the vibrational energy of the molecules of the sample were examined by X-ray diffraction (XRD) and Fourier Transform Infrared Spectroscopy measurements. UV-Vis spectroscopy was used for measurement of optical properties of FTO/SnO_2/ZnO films.

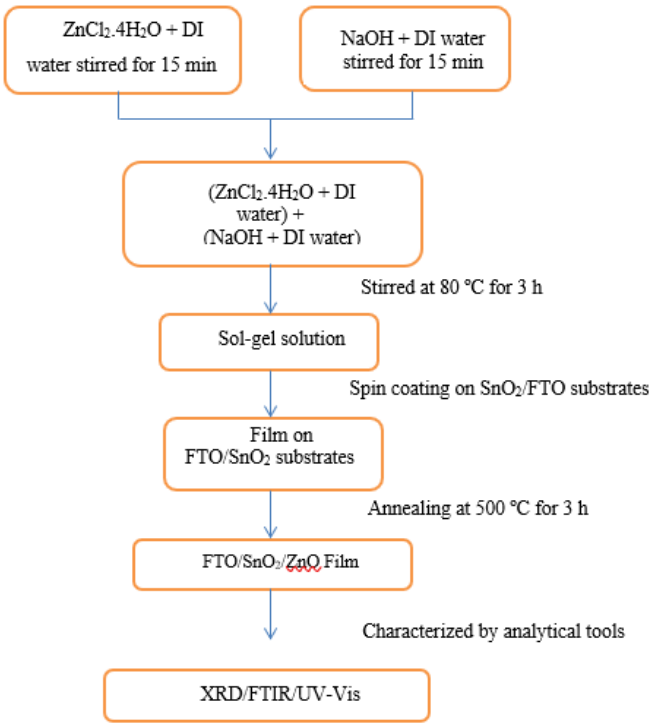

Figure 3 Experimental procedures of ZnO and Device Fabrication FTO/ SnO_2/ZnO films

Results and Discussion

XRD Analysis of SnO_2/ZnO Films

The structural properties of sol-gel synthesized SnO_2/ZnO films were determined by using XRD method. According to XRD results, the distinct peaks at 2θ values of 20.98º and 37.76º, which were assigned to indices (110) and (200) crystal planes. They can be indexed as a tetragonal crystal structure of SnO_2 by matching with the Joint Committee on Powder Diffraction Standard (JCPDS) card number 00-046-1088. The diffraction peaks at 2θ = 25.12º, 28.92º, 32.82º, 43.98º, 64.34º and 67.10º correspond to the crystalline planes (101), (100), (102), (103)

and (201) respectively. These results were in good agreement with of hexagonal crystal structure ZnO phases according to the JCPDS card number 00-065-0725. The XRD analysis revealed that all of the characteristic peas in these spectra were the evidence of the coexistence of both tetragonal SnO_2 and hexagonal ZnO crystal structures in the samples (K. Wongsaprom, A. Winyayong, S. Maensiri, 2018). The sharp and narrow peaks in all spectra implied that the samples have high crystallinity degrees. These XRD spectra indicated that the SnO_2/ZnO films were successfully synthesized using sol-gel method. The XRD pattern comparison of SnO_2/ZnO films with different molar ratios was shown in figure 4. Table (1-5) listed the structural properties and average crystallite sizes of SnO_2/ZnO films with different ratios. According to these results, the average crystallite sizes were decrease with increasing molar ratios.

Table 1. Structural properties and average crystallite sizes of SnO_2/ZnO films (S-1)

(hkl)	2θ (deg)	FWHM (deg)	Crystallite size (nm)
(110)	20.98	0.57353	14.08
(101)	28.92	0.15292	53.64
(200)	37.76	0.24967	33.62
(102)	43.98	0.26078	32.84
(103)	64.34	0.33955	27.63
Average crystallite size			32.36

Table 2. Structural properties and average crystallite sizes of SnO_2/ZnO films (S-2)

(hkl)	2θ (deg)	FWHM (deg)	Crystallite size (nm)
(110)	20.98	0.5385	15.01
(101)	28.92	0.25959	31.59
(200)	37.76	0.25526	32.88
(102)	43.98	0.26887	31.86
(103)	64.34	0.20830	45.04
Average crystallite size			31.27

Table 3. Structural properties and average crystallite sizes of SnO_2/ZnO films (S-3)

(hkl)	2θ (deg)	FWHM (deg)	Crystallite size (nm)
(110)	20.98	0.58812	13.73
(101)	32.78	0.21856	37.88
(200)	37.74	0.25407	33.03
(102)	43.98	0.2493	34.36
(103)	64.34	0.32317	29.03
(201)	67.14	0.24508	38.89
Average crystallite size			31.15

Table 4. Structural properties and average crystallite sizes of SnO_2/ZnO films (S-4)

(hkl)	2θ (deg)	FWHM (deg)	Crystallite size (nm)
(110)	20.98	0.58334	13.84
(101)	25.12	1.02822	7.914
(100)	32.82	0.23081	35.87
(200)	37.76	0.26234	31.99
(102)	43.98	0.25125	34.09
(103)	64.34	0.30314	30.95
(201)	67.1	0.20903	45.59
Average crystallite size			28.61

Table 5. Structural properties and average crystallite sizes of SnO_2/ZnO films (S-5)

(hkl)	2θ (deg)	FWHM (deg)	Crystallite size (nm)
(110)	20.98	0.55183	14.63
(101)	28.92	0.25759	31.84
(200)	37.76	0.24872	33.75
(102)	43.98	0.26108	32.81
(103)	64.34	0.36817	25.48
Average crystallite size			27.70

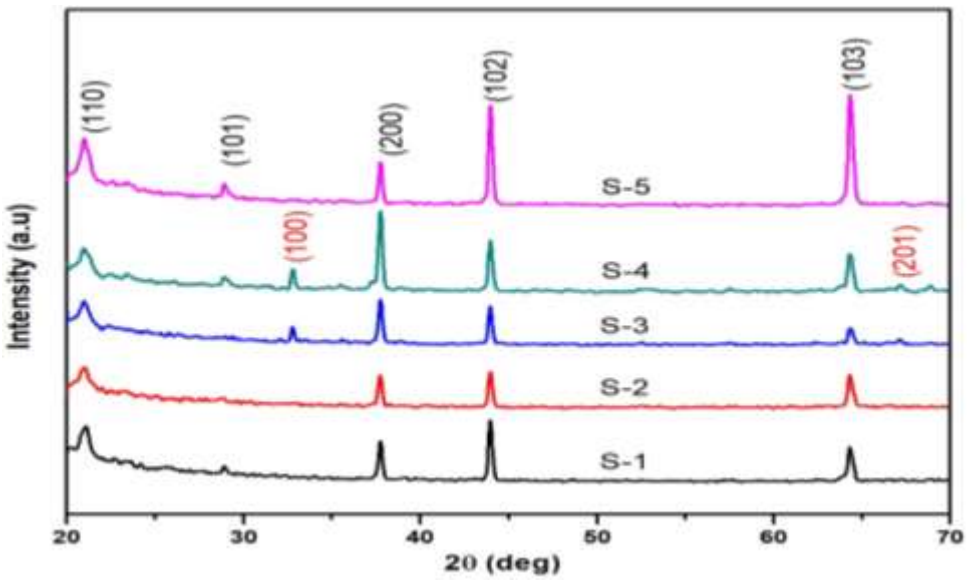

Figure 4 Comparison of XRD patterns of SnO_2/ZnO films

FTIR Analysis of SnO_2/ZnO Films

The functional groups of the sol-gel synthesized SnO_2/ZnO films investigated using FTIR spectroscopy. The spectra of SnO_2/ZnO films have strong and broad bands at ~3360 cm^{-1} peak that are related to O-H stretching of water molecules adsorbed on the surface of the synthesized materials. Similarly, another strong band at ~1630 cm^{-1} peaks assigned to O-H bending vibration of hydroxyl group. The weak bands observed at ~2000-2500 cm^{-1} were C ≡ C stretching vibration of alkyne. The finger prints region of metal oxygen bond showed the characteristic absorption bands in the wave number region 400 cm^{-1} to 800 cm^{-1} (L. Motelica, O. Oprea, B. Vasile, et al.,2023). In this study, the absorption peaks of O-Sn-O stretching vibration were observed at ~649-689 cm^{-1} and the absorption peaks of Zn-O stretching vibration were observed at ~437-465 cm^{-1} respectively (Z. Khatoon, H. Fouad, H. K. Seo, et al.,2020). The comparison of FTIR spectra for SnO_2/ZnO films with different molar ratios was shown in figure 5.

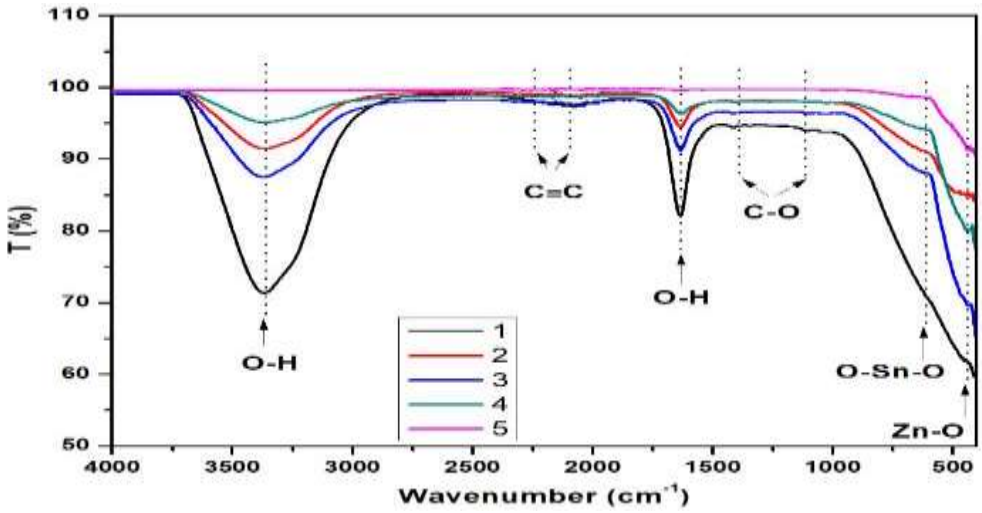

Figure 5. Comparison of FTIR spectra for SnO_2/ZnO films with different molar ratios

UV-Vis Analysis of SnO_2/ZnO Films

The UV-Vis spectra of all films were obtained on UV-Vis spectrometer in the range of 200 nm -700 nm. Figure 6 (a-e) showed that the UV-Vis absorption spectra of SnO_2/ZnO electron transport layer (ETL) films with different molar concentrations. It was found that the maximum absorption of wavelength obtained by coating onto FTO is in the ultraviolet region. The wavelength ranges of spectrum laid between 200 nm to 400 nm. There are different methods to obtain the optical band gap of the thin films. Here, the Tauc's plot method is used to obtain the band gap of the SnO_2 films with different molar concentrations. The $(\alpha h\upsilon)^2$ and $h\upsilon$ characteristic curve of SnO_2/ZnO ETL films with different molar concentrations were listed in Table 6. On the characteristic curve, the extrapolating the straight line onto horizontal axis ($(\alpha h\upsilon)^2 = 0$), give the values of band gap and the obtained films had the direct band gap of 3.44 eV, 3.47 eV, 3.53 eV, 3.55 eV and 3.58 eV with different molar concentrations respectively.

Table 6 Observed energy bandgaps and referenced energy bandgaps

Samples	E_g (for 2 layers) (This study)	E_g (for SnO_2 only) (previous study)	References
S-1	3.44 eV	3.95 eV	3.2-3.6 eV
S-2	3.47 eV	3.93 eV	
S-3	3.53 eV	3.93 eV	
S-4	3.55 eV	3.94 eV	
S-5	3.58 eV	3.97 eV	

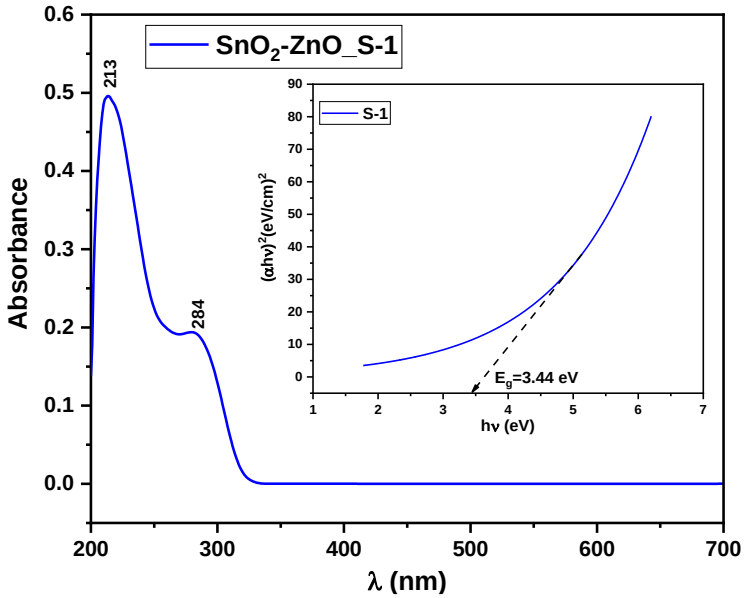

Figure 6 (a) UV-Vis absorption spectrum and energy band gap of SnO_2/ZnO film (S-1)

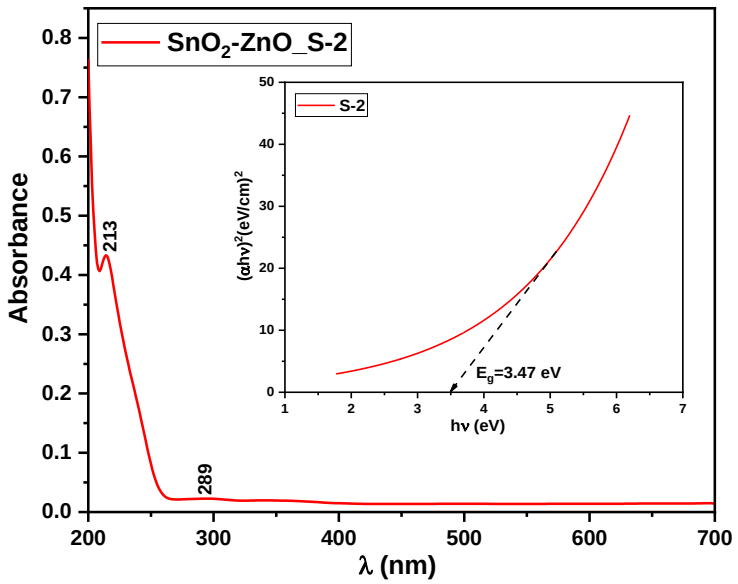

Figure 6 (b) UV-Vis absorption spectrum and energy band gap of SnO_2/ZnO film (S-2)

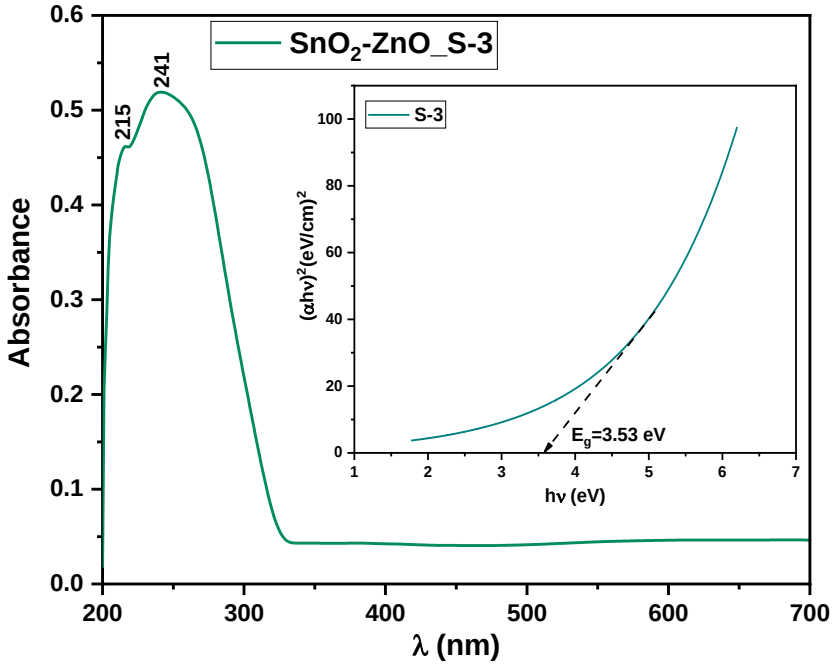

Figure 6 (c) UV-Vis absorption spectrum and energy band gap of SnO_2/ZnO film (S-3)

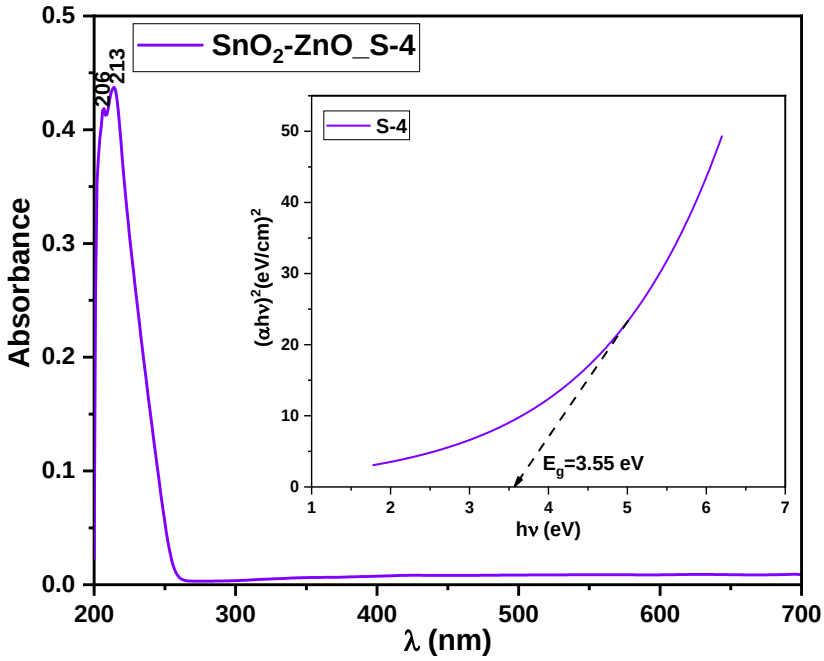

Figure 6 (d) UV-Vis absorption spectrum and energy band gap of SnO_2/ZnO film (S-4)

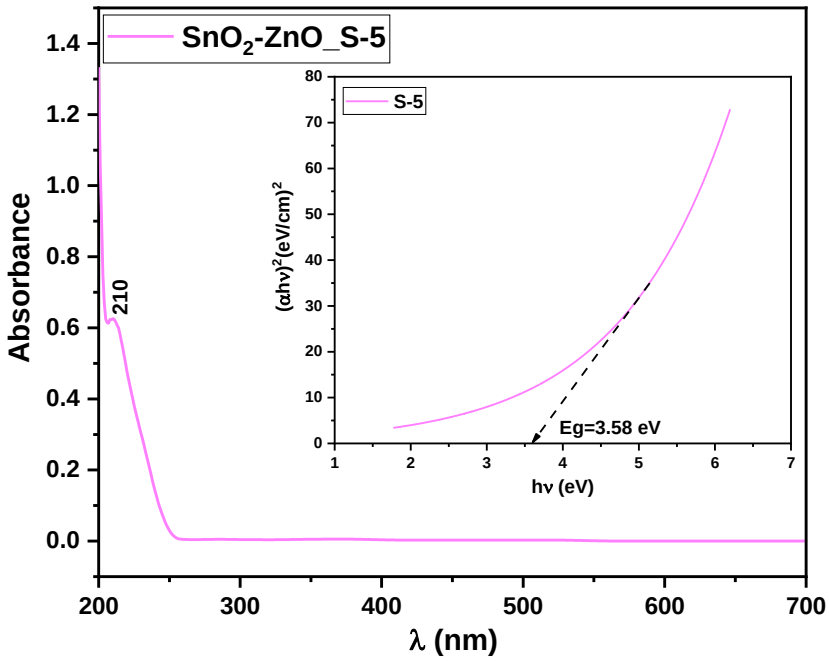

Figure 6 (e) UV-Vis absorption spectrum and energy band gap of SnO_2/ZnO film (S-5)

Conclusions

The suitable synthesis of SnO_2/ZnO films through sol-gel spin coating at varying molar ratios was examined by XRD analysis, indicating the presence of both SnO_2 and ZnO structures with distinct crystalline patterns. The XRD results further indicated a reduction in grain size with increased molar concentration. FTIR analysis highlighted specific absorption peaks, including O-Sn-O (~649-689 cm-1) and Zn-O (~437-465 cm-1), providing insights into the chemical bonding within the deposited films. UV-Vis results indicated energy band gap values closely aligned with reported values (3.2-3.6 eV) (S. Dániel, S. Tamas, D. Imre, et al., 2009). These findings collectively suggest the potential of SnO_2/ZnO layers as effective electron transport layers (ETL) in perovskite solar cells, thereby enhancing overall performance.

Acknowledgments

We wish to express our deepest gratitude to Dr Tin Maung Tun, Rector, University of Yangon, for his encouragement to submit this paper. We are very grateful to Professor Dr Yin Maung Maung, Head of Department of Physics, University of Yangon, for his kind encouragement. We would like to express our sincere thanks to Dr Ye Chan, Professor and Head, Universities' Research Center, and Professor Dr Cho Cho Thet, Department of Physics, University of Yangon, for their valuable advice to this paper.

References

Aoki, A., Sasakura, H.: Tin oxide thin film transistors. Japan J. Appl. Phys. 9,582,1970.

Chopra, K.L., Major, S., Pandya, D.K.: Transparent conductors–a status review. Thin Solid Films 102, 1, 1983.

Cheng, B., Russell, J.M., Shi, W., Zhang, L., Samulski, E.T.: Large-scale, solution phase growth of single-crystalline SnO2 nanorods. J. Am. Chem. Soc. 126, 5972, 2004.

Du, F., Guo, Z., Li, G.: Hydrothermal synthesis of SnO2 hollow microspheres. Mater. Lett. 59, 2563, 2005.

Duan, J., Yang, S., Liu, H., Gong, J., Huang, H., Zhao, X., Zhang, R., Du, Y.: Single crystal SnO2 zigzag nanobelts. J. Am. Chem. Soc. 127, 6180, 2005.

Dai, Z.R., Gole, J.L., Stout, J.D., Wang, Z.L.: Tin oxide nanowires, nanoribbons, and nanotubes. J. Phys. Chem. B 106, 1274, 2002.

Fujihara, S., Maeda, T., Ohgi, H., Hosono, E., Imai, H., Kim, S.: Hydrothermal routes to prepare nanocrystalline mesoporous SnO2 having high thermal stability. Langmuir 20, 6476, 2004.

G. Lamdhade, F.C. Raghuwanshi, R.M. Agrawal, V.M. Balkhande, T. Shripathi, "SnO_2 Nanoparticles Synthesis Via Liquid-Phase Co-Precipitation Technique," *Adv. Mater. Lett*. 6, 738–742, 2015.

Hu, J.Q., Ma, X.L., Shang, N.G., Xie, Z.Y., Wong, N.B., Lee, C.S., Lee, S.T.: Large scale rapid oxidation synthesis of SnO2 nanoribbons. J. Phys. Chem. B 106, 3823, 2002.

K. Wongsaprom, A. Winyayong, S. Maensiri, "Synthesis and room-temperature ferromagnetism in flower-like SnO_2 nanostructures," *J. Phys. Conf. Ser*. 1144, 012042, 2018.

Liu, Y., Koep, E., Liu, M.: A highly sensitive and fast-responding SnO2 sensor fabricated by combustion chemical vapor deposition. Chem Mater 17, 3997, 2006.

L. Motelica, O. Oprea, B. Vasile and A. Ficai, "Antibacterial activity of solvothermal obtained ZnO nanoparticles with different morphology and photocatalytic activity against a dye mixture," *Int.J.Mol.Sci*.245677, 2023.

M-G. Kim, M. G. Kanatzidis, A. Facchetti, and T. J. Marks, Nature Materials 10, 2002.

Perovskite, S. Cell, and M. Karolus, "Hybrid Mesoporous TiO 2 /ZnO Electron Transport Layer for Efficient Perovskite Solar Cell," 2023.

Peng, Z., Shi, Z., Liu, M.: Mesoporous Sn–TiO2 composite electrodes for lithium batteries. Chem. Commun. 21, 25, 2000.

Paraguay-Delgado, F., Antúnez-Flores, W., Miki-Yoshida, M., Aguilar-Elguezabal, A., Santiago, P., Diaz, R., Ascencio, J.A.: Structural analysis and growing mechanisms for long SnO2 nanorods synthesized by spray pyrolysis. Nanotechnology 16, 688, 2005.

Pourfayaz, F., Khodadadi, A., Mortazavi, Y., Mohajerzadeh, S.S.: SnO2 sensor selective to ethanol in presence of CO, LPG and CH4. Sensors Actuators B 108, 172, 2005.

P.A. Luque, O. Nava, C.A. Soto-Robles, M.J. Chinchillas-Chinchillas, H.E. Garrafa-Galvez, Y.A. Baez-Lopez, K.P. Valdez-Núñez, A.R. Vilchis-Nestor, A. Castro-Beltrán, "Improved photocatalytic efficiency of SnO2 nanoparticles through green synthesis," *Optik*, 206, 164299, 2020.

S. Chen, Z. Sun, L. Zhang, H. Xie, "Photodegradation of Gas Phase Benzene by SnO_2 Nanoparticles by Direct Hole Oxidation Mechanism," *Catalysts*, 10, 117, 2020.

S. Dániel, S. Tamas, D. Imre, "Optical properties of zinc peroxide and zinc oxide multilayer nanohybrid films," *Appl. Surf. Sci*, 255, 6953−6962, 2009.

W. Zhou, Y. Y. Liu, Y. Z. Yang, P. Wu, "Band Gap Engineering of SnO2 by Epitaxial Strain: Experimental and Theoretical Investigations," *J. Phys. Chem. C*, 118, 6448−6453, 2014.

Z. Khatoon, H. Fouad, H. K. Seo, et al, "Sensing biomarkers of lung cancer feasibility study of doped SnO_2 nanomaterial for electronic nose towards sensing biomarkers of lung cancer," *J.Mater.Sci.:Mater. Electron*.3115751–63, 2020.